Design of Single Camera 3D Laser Scanning System Based on Artificial Intelligence

Wen-da Xie[1] and Qing-bang Zeng[2(✉)]

[1] Computer Engineering Technical College (Artificial Intelligence College), Guangdong Polytechnic of Science and Technology, Zhuhai 519090, China
wowogogo22@yeah.net

[2] College of Information Engineering, Jiangmen Polytechnic, Jiangmen 529000, China
honda455@163.com

Abstract. At present, the binocular/multi-visual 3D laser scanning system needs to register and match the acquired images, and needs to calibrate and calibrate frequently, which is easy to cause errors. In the hardware design, we choose the model and parameter of camera, laser, stepper motor and its driver. In the software design, we use octree structure to index the 3D data tree structure, preprocess the scanning data, introduce artificial intelligence scanning algorithm, design the optimal hyperplane based on SVM to complete the noise recognition, and finally extract the scanning image features to complete the design of the whole scanning process. Experimental results show that, compared with the traditional system, the light stripe obtained by the design system is complete, and the ranging result is more close to the actual distance.

Keywords: Artificial intelligence · Monocular vision · 3D laser scanning · System design

1 Introduction

The 3D laser scanning system integrates the knowledge of optics, machinery, electronic control, image processing, computer graphics and many other fields into one, which can quickly obtain the 3D point cloud data of the object surface. 3D acquisition methods are generally divided into contact measurement and non-contact measurement. The basic principle of 3D laser scanning measurement is as follows: Laser stripes are formed when the laser is irradiated to the surface of the object to be measured. 3D information of laser stripes is extracted from the images taken by the cameras on the left and right sides. The laser generator and the cameras rotate synchronously around the object to obtain 3D coordinate data of the surface of the object to be measured quickly. At present, it is a hotspot in the field of computer vision to reconstruct 3D models of objects and environments by using computers. In the mid- nineties of the twentieth century, an advanced high-precision automatic stereo scanning technology - three-dimensional laser scanning technology appeared in people's vision. This new technology, also known as

S. Wang et al. (Eds.): IoTCare 2021, LNICST 415, pp. 233–248, 2022.
https://doi.org/10.1007/978-3-030-94182-6_17

"Scene Reproduction Technology", integrates optical, mechanical, electrical and computer technologies, and is mainly used to describe the shape, structure and color of space objects, so as to model and reconstruct the shape of objects with high accuracy.

As the main equipment of obtaining 3D information in reverse engineering, laser 3D scanning system is widely used in mechanical CAD system and NC machining, film and TV stunt making based on virtual reality, archaeological survey and virtual museum for the purpose of protecting cultural relics, costume design and 3D communication. Since the 1980s, with the rapid progress of information technology, laser 3-D scanning equipment has been developing towards the direction of low cost, high precision, high speed, easy operation and portability [1, 2]. At present, in order to ensure the scanning speed, the binocular/multi-visual 3D laser scanning system is usually used. Reference [3] proposed a virtual reconstruction system of building space structure based on laser 3D scanning, and designed the overall reconstruction system according to single-chip microcomputer mapping and 3D laser scanning technology. The process, preprocessing and registration method of obtaining building spatial structure data by laser 3D scanning are analyzed in detail. Three-dimensional reconstruction of architectural spatial structure model is carried out by using triangular mesh. The external space acquisition tool and interactive editing environment are provided for the operator to realize the virtual reconstruction of the architectural space structure. The experimental results show that the virtual reconstruction of building space structure can be realized by using this system. The 3D modeling results have high fitting degree with the actual results, short modeling time and strong applicability. Reference [4] proposed the pavement deformation analysis method based on 3D laser scanning point cloud, and used the point cloud data obtained by 3D laser scanning technology to operate the road surface. The road surface and digital model established qu2alitative and quantitative analysis of the pavement deformation, and then the overall deformation area and deformation of the road surface. The results show that the 3D laser scanning technology can make the road digital analysis more intuitive and simple, which is of great significance to the automatic development of road disease monitoring technology. In the process of using, the images acquired need to be registered and matched, which is easy to cause errors and need to be calibrated and calibrated frequently. Therefore, this paper designs a single camera 3D laser scanning system based on artificial intelligence, to improve the scanning accuracy. The innovation of the single camera 3D laser scanning system based on artificial intelligence is to use the artificial intelligence scanning algorithm to design the optimal hyperplane based on support vector machine to complete noise identification. The experimental results show that the designed system can obtain a more complete light strip, and the ranging result is closer to the actual distance, which is of great significance to the actual 3D laser scanning.

2 Design of Single Camera 3D Laser Scanning System Based on Artificial Intelligence

2.1 Hardware Design

In the process of system design, the structure of 3D laser scanning system is different because of different application environment and different principle of scanning and

imaging. The 3D laser scanning system designed in this paper generally consists of a high precision and high speed laser transmitter, a set of reflecting prisms and a built-in digital camera (which can obtain digital images of objects in front of the camera). Objects can be scanned in all directions by the rotation of the tilt, and a group of scanning point clouds can be obtained by processing and integrating the acquired data. Monocular vision is usually considered as an ideal pinhole projection model, which can describe the relationship between the coordinate of 3-D points and the relative 2-D points in the image plane. The system described in this paper makes full use of the geometry of pinhole projection model to construct an efficient 3D laser scanning system. The scanning system consists of a horizontal template, in order to obtain high precision data points, the instrument used must be of high precision. In the hardware design of the system, the hardware part is designed.

Select the Camera

The following factors shall be taken into consideration when selecting the type of camera: (1) The resolution of the camera shall not be lower than 680 × 480, and the frame rate shall not be lower than 30fps at this resolution; (2) The brightness, gray level, white balance and other parameters of the image may be adjusted, and the interference light may be filtered; and (3) The size of the picture taken by the camera shall meet certain requirements. Taking the above factors into consideration, the SONY Effio-E 4140+673 CCD camera is selected. The main technical parameters of the camera are listed in Table 1:

Table 1. Camera parameters

Name	Parameter	Company
Camera pixel	More than 380,000	/
Signal to noise ratio	48/58	dB
Color imaging	Colour to black	/
White balance mode	Automatic	/
Resolution	700	TVL
Focusing mode	Autofocus	/
Lens	DC lens	/
Others	Backlight compensation	/

The camera can be dynamic detection, manual digital noise reduction, backlight compensation, and the picture clear in line with the system requirements.

Selective Laser

When selecting a laser, the projection angle of the line laser should be considered first to ensure that the length of the laser line projecting to the object should be at least 800 mm when the projection distance is 600 mm. In addition, select a slightly more powerful

laser, so that the projection of the laser line will be more thin, improve the accuracy of modeling. And to choose stable light intensity, less scattering of the line laser [5, 6]. The optical fiber laser has been widely used in laser radar, laser ranging and imaging because of its high photoelectric conversion efficiency, good thermal and mechanical stability, compact structure and good output beam quality. Pulsed laser has higher peak power than CW laser and can transmit long distance. Therefore, pulsed laser is often used in the detection of long-range targets. For laser 3D imaging, the pulse width of laser pulse determines its radial resolution.

According to the above rules, the system selects the invisible infrared laser. It is required that the laser should meet the requirement of high quality in 110° sector and the laser intensity distribution should be uniform. Table 2 lists the main parameters of the lasers used in the system:

Table 2. Main parameters of line laser

Name	Parameter	Company
Output wavelength	1021	±nm
Operating voltage	4.3–5	VDC
Angle of line	110	°
Facula diameter	Adjustable	mm
Output power	100	mW
Working current	<180	mA
Facular focusing	Adjustable	/
Mode of operation	Continuous laser	/

Under the conditions of the above parameters, it is necessary to verify whether the length of the line laser meets the requirements. The calculation formula of linear laser is:

$$L_x = L_t \times \tan\frac{\theta}{2} \tag{1}$$

In the formula, L_x represents the length of the line laser that can be projected, L_t represents the projection distance of the laser, and θ represents the line angle degree. In this paper, the length of line laser is required to be more than 800 mm. Through algebraic calculation, it can be seen that the selected laser can meet the requirements of the system.

Selecting Step Motor and Its Driver

The objective of this paper is to build a 3D map model of the surrounding environment, so the camera and the line laser are required to rotate at 360°. Therefore, in the design of the 3D laser scanning system, the camera and the line laser are fixed into an adjustable whole by mechanical structure, and then fixed to the axis of the stepping motor. In the choice of stepper motor requires stepper motor to be able to rotate in 360° range, and motor speed

adjustable, in order to facilitate system debugging [7, 8]. The choice of motor driver must match the two-phase four-wire stepper motor, and the selected driver must also be two-phase output. For the convenience of motor adjustment, the choice of current subdivision and drive can be adjusted [9, 10]. In order to save costs, the laboratory has selected the existing stepper motor, model 57BYGH7630, the system choice of stepper motor driver for the DM542A subdivision type two-phase hybrid. Table 3 shows the main technical parameters of the stepper motor and driver:

Table 3. Parameters of stepping motor and its driver

Classification	Name	Parameter	Company
Stepping motor	Stepping angle	1.8	°
	Static moment	2.0	N·m
	Moment of inertia	480	$g \cdot cm^2$
	Lead wire	6	Root
	Phase voltage	3.0	V
	Phase current	3.0	A
Stepping motor driver	Input voltage	24–50	VDC
	Input current	<2	A
	working temperature	−10–48	°C
	Output current	1.0–4.2	A
	Consumption	80	W
	Weight	200	g

Subdivided two-phase hybrid stepper motor driver DM542A power supply mode for DC power supply, supply voltage of 16–50 V. It is suitable for stepper motor type: The outer diameter is 42–86 mm, 1850 V drive voltage, current less than 4.0 A two-phase hybrid. This driver uses the AC servo driver current loop for subdivision control, motor torque fluctuation is very small, low speed operation is very smooth, almost no vibration and noise. At high speed, the torque is much higher than that of other two-phase actuators [11, 12]. The actuator is widely used in high resolution equipment, such as packaging machinery, CNC machine tools, engraving machines, etc. In order to make the motor run more stably, the decelerating gear is equipped in the 3D laser scanning system. The deceleration gearbox model is 06AG 15, its deceleration ratio is 1:15. At this point completed the design of the hardware part.

2.2 Software Design

Scan Data Preprocessing

In the 3D laser scanning system, the pulse data sent by the laser equipment must be received first. With the support of the hardware structure designed in this paper, the

scanned image has a large amount of point cloud data, and the arrangement is chaotic. So we need to preprocess the data. First, the receiving channel is designed. In the receiving channel, the drift error can be corrected by measuring the amplitude of the pulse, and then a lookup table is used to correct the result [13]. The time of arrival of the pulse is generated by the rising edge of the pulse, so the large pulse does not affect the determination of the time of arrival of the pulse. The measurement of the pulse amplitude is achieved by using two identical peak detectors. The first peak detector is placed behind the preamplifier, and the second peak detector is placed behind the post-stage amplifier. This configuration maximizes the compensation range. For weak signals, the second peak detector is used to compensate, because at the small signal level, the compensation is sensitive to variations in the amplitude of the small signal [14, 15]. When the second peak detector is saturated, the amplitude information from the first peak detector is available because the first peak detector is still in the linear region. By the time the first peak detector is saturated, the signal is very large, but the arrival time of the pulse is insensitive to the large signal, so saturation is not a big problem in the early stage of data processing, the relationship between the discrete points can be established by building a point cloud spatial index. This article uses an octree structure to index the 3-D data tree. The example image is shown Fig. 1:

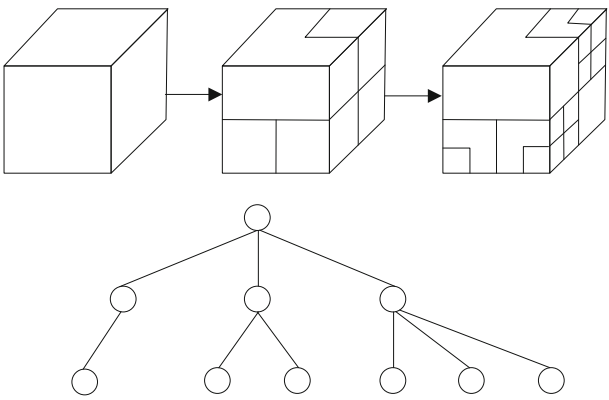

Fig. 1. Octree diagram

Octree is an extension of data structure based on binary tree of one-dimensional data and quadtree of two-dimensional data. Each node of octree is divided by a cube. This division method is based on the line segment of binary tree and the rectangle of quadtree. This stereo partitioning allows an octree to have up to eight child nodes corresponding to each partitioned cube node on the octal rectangle. When a node has no children, it means that the node can evenly represent the corresponding space without further subdivision [16, 17]. The storage point of 3-D point cloud belongs to dimensionless technology. That is to say, its state is a particle in space, and its corresponding volume can not be calculated [18]. When using octree to search, the nearest node is found, and the nearest neighbor is searched to approximate the three splitting planes.

After the relationship between discrete points is established, the noise of the original point cloud data should be eliminated. Based on the characteristics of vehicle radar point cloud data, it is necessary to reorganize the original data to compress the original data, which can be voxelized to achieve denoising. A cube in an octree can represent a voxel, and the cube can record the location of the voxel. The location information can be expressed as (r, c, h), and the calculation formula is as follows:

$$r=\frac{x-x_{\min}}{v},\ c=\frac{y-y_{\min}}{v},\ h=\frac{z-z_{\min}}{v} \tag{2}$$

The location information (r, c, h) of voxel respectively represents the distance between voxel and the smallest x, y, z and location point in all point clouds. $x_{\min}$, $y_{\min}$ and $z_{\min}$ are the minimum values of x, y and z. The number of points recorded in voxels will exist in the range or boundary of voxels. In this way, the relationship between point cloud and voxel is established to complete the scanning data preprocessing.

Introduction of Artificial Intelligence Scanning Algorithm

After getting the preprocessed scanning image, it is necessary to automatically diagnose the noise in the scanning process [19]. This paper uses a typical optimized dynamic time warping algorithm to express the relationship between the collected signal and the reference signal. In the process of diagnosis, assume that the reference signal is expressed as Q and the acquisition signal is expressed as C, then:

$$\begin{cases} Q = q_1, q_2, \ldots q_i, \ldots, q_n \\ C = c_1, c_2, \ldots c_j, \ldots, c_m \end{cases} \tag{3}$$

In the formula, n represents the length of Q, that is, the number of frames of the image, q_i represents the characteristic value of the i frame, and m represents the length and number of frames of C. When the length between the acquisition signal and the reference signal is the same, the distance between them can be calculated directly, and the dynamic time warping method is needed. Firstly, a matrix with dimension $n \times m$ is constructed. Any element in the matrix can represent the distance between q_i and c_i. In distance calculation, Euclidean distance is used as the calculation basis. While representing the distance, it can also reflect the similarity between two points. The dynamic time warping algorithm mainly finds Q and C through the optimal path:

$$W = w_1, w_2, \ldots, w_{\mathrm{k}}, \max(m,n) \le k < \mathrm{m}+\mathrm{n}-1 \tag{4}$$

In the formula, W represents the optimal path, and the k element in W can be defined as $w_{\mathrm{k}} = (i, j)_k$, which is constrained by boundary conditions, continuity and monotonicity. In order to minimize the structural risk, this paper uses SVM to map the image samples to the high-dimensional feature space, and constructs the noise data of the image into the optimal hyperplane by support vector, as shown in Fig. 2:

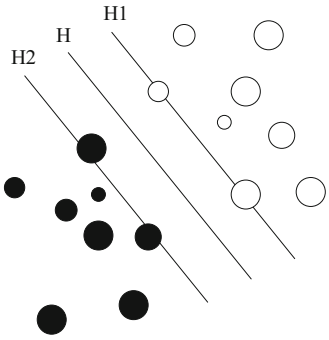

Fig. 2. Optimal hyperplane based on SVM

In the above picture, black circle and white circle represent two kinds of samples, which are divided into two kinds of noisy data and non-noisy data, and are used to construct the optimal hyperplane. In the process of constructing the optimal hyperplane, there are:

$$\begin{cases} \min\limits_{w,b} \frac{1}{2}\|p\|^2 \\ s.t.\ \ y_i(p \cdot x + b) \geq 1,\ i = 1, 2, ..., l \end{cases} \tag{5}$$

In the formula, p is the normal vector and b is the threshold. Through the above formula, we can get the image stripe features of noise data and non noise data in different working modes, and treat these data as training data through support vector machine [20, 21]. After inputting the data to be tested into the support vector machine, it is compared with the training data samples. For the scanning system designed in this paper, a variety of indicators will be involved in the noise recognition process [22]. The image noise recognition in the scanning system can be represented by the multi indicator factor set U, that is, the geometric domain of evaluation indicators. Therefore, the noise recognition reference index set can be represented by V, Then the two sets can be expressed as follows:

$$U{=}\{u_1, u_2, \ldots, u_n\},\ V = \{v_1, v_2, \ldots, v_n\} \tag{6}$$

For the weighted evaluation of noise recognition, it is necessary to establish the fuzzy vector A of weight allocation, that is, the index weight set. The fuzzy relationship of the product of the multi index factor set U and the noise recognition reference index set V can be expressed by R, which is in the form of fuzzy matrix. The membership function between the index and the evaluation level can be obtained, and the matrix multiplication of A and R can be obtained

$$T^*{=}\left(t_1^*, t_2^*, \ldots, t_n^*\right) \tag{7}$$

The final noise recognition result Q can be expressed as:

$$Q = T^* \times P' \tag{8}$$

In the formula, P' is transpose matrix, so as to complete the automatic diagnosis of scanning image noise.

Extraction of Scanning Image Features

In order to extract the information of 3D laser scanning target accurately and effectively, we must distinguish it from other objects according to the characteristics of the target. In some complex scenes, in order to achieve the precise scanning of the target, we need to filter out the objects except the target objects. In the process of clustering, eigenvectors are associated with each point, and in eigenvectors, geometric radiometric values are also included. Clustering is to filter out the low point cloud, and then set up the horizontal grid after projection. Mark the grid as 0 for the grid with point clouds and null for the grid without point clouds. In the neighborhood, the grid containing the point cloud will be grouped into the same cluster block and a new natural number will be re-assigned as a marker. The grid diagram after clustering is shown in Fig. 3:

Null	Null	Null	Null	Null	Null	Null	Null	Null	Null	Null	Null
Null	1	1	Null	Null	Null	Null	Null	Null	Null	5	5
Null	1	1	1	Null	Null	Null	4	Null	Null	5	5
Null	Null	Null	1	Null	Null	Null	4	Null	Null	5	5
Null	Null	Null	Null	Null	Null	4	4	4	Null	5	5
Null	2	2	Null	Null	4	4	4	Null	Null	5	5
Null	2	2	2	Null	Null	Null	4	Null	Null	5	5
Null	2	2	2	Null	Null	Null	Null	Null	Null	5	5
Null	Null	2	Null	Null	Null	Null	Null	Null	Null	5	5
Null	Null	Null	Null	3	3	3	Null	Null	Null	5	5
Null	Null	Null	3	3	3	3	Null	Null	5	5	5
Null	Null	Null	Null	3	3	Null	Null	Null	Null	Null	Null

Fig. 3. Cluster diagram of scanning target

After clustering, we can see some clustering blocks, but a clustering block does not represent the same kind of point cloud, in the subsequent feature extraction, we need to remove other objects together with the object. According to this characteristic, a plane can be intercepted at 1.3–1.5 m from the ground, and the point clouds of the upper and lower parts of the object can be projected horizontally and meshed. After the large clustering unit is obtained, the projection area of the upper and lower part of the point cloud is calculated, the projection span is calculated, and the 3D information of the object is extracted. The scan process is shown in Fig. 4:

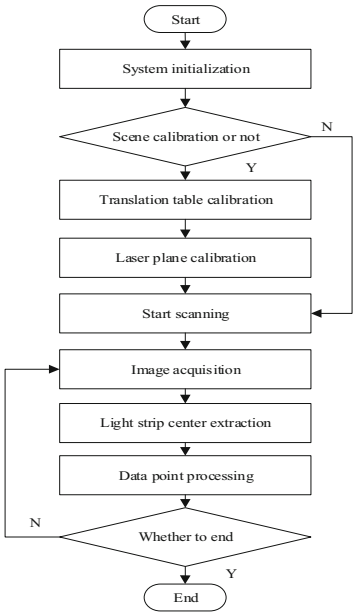

Fig. 4. Workflow of a scanning system

Before the system starts to run, it is necessary to complete the calibration of the camera, obtain the camera focus, imaging origin, distortion coefficient and other information. The initialization phase reads camera calibration data from an XML file that has been written, as well as the calibration data of the original translation table and the laser. The CCD image acquisition stage completes the automatic correction of the acquired image. In the phase of parameter acquisition, the laser plane calibration is performed and the translation velocity of the translation table is obtained. At the beginning of the scan phase, start the translation station to determine the location of the scan data points. In the scanning stage, the light stripe center is extracted and the 3D projection transformation is completed to obtain the point cloud data. When the light strip removes the scanning area, the system automatically terminates the scan, or manually terminates the scan. After scanning, it is necessary to correct the error. Due to the propagation of laser pulses in atmosphere or the interaction between laser pulses and target, the shape and amplitude of receiving pulses are different from those of transmitting pulses. Therefore, it is difficult to determine the time of arrival of the pulse, which has an effect on the ranging results. The error caused by the discrimination of the time reaching the pulse is called drift error. The function of time discrimination is to change the input analog pulse signal into logic signal by locating the pulse arrival time. Another is to extract the useful signal from the noise. At present, there are three kinds of identification methods: frontier identification method, zero-crossing comparison method, also known as high-pass capacitance identification and constant ratio timing method. The above principle methods have their own advantages and disadvantages, according to different applications to choose which method to use. In addition to drift errors due to changes in the

amplitude and shape of the received signal, there are also errors due to temperature and service time and measurement errors due to noise.

3 System Experimental Test

3.1 Build a Test Environment

According to the structure, hardware and software of the system, the image acquisition system, line laser and control turntable system are connected with the computer, and set up on the designed and assembled robot test prototype. Collect data on a dataset, which has the advantage that most conversations are public, which means that a lot of data is available through its API. A collection of open data sets contributed by data scientists involved in machine learning projects.The experimental environment was scanned by controlling the step motor to drive the camera and the laser, and the scanning process was filmed into the computer. After the video is processed by computer, the reconstructed 3D model is displayed. After the completion of the system to carry out system debugging, mainly divided into the following steps:

(1) Camera debugging: adjust the camera's parameters such as the angle of view, resolution, brightness, framing, saturation, contrast, backlight compensation, and white balance, turn off the camera's functions such as automatic gain control, automatic color compensation, and automatic weak light compensation, and then calibrate the camera; (2) step motor debugging: use the step motor controller to program and control the motor rotation, make the motor rotate uniformly, and collect the image of the scanned area; and (3) line laser debugging: control the angle between the camera spindle plane and the line laser plane to be controlled at 30. Between 600 and 600 to ensure measurement accuracy.

After the system is built and debugged, the scanning measurement can be started. In the process of scanning measurement, we should try our best to ensure the environment without light interference. When using 3D laser rangefinder to construct 3D model, the characteristic of point cloud data is different for different objects, so the method and process of data processing are also different. After the data acquisition, data processing, including: data acquisition, data smoothing, denoising, data model reconstruction and visualization. In the whole process, the camera calibration, system debugging is the premise of the measurement experiment, and is also the key to improve the accuracy of the system. The data processing process provides reliable point cloud data for 3D model reconstruction, which can ensure the accuracy and speed of the whole system. This system performance test runs under the Windows XP system, using VS2008, OpenCV and OpenGL's open source function library compilation. During the experiment, the scanning process is filmed as video, and then the video frames are extracted offline for processing, which can facilitate the debugging and save the experimental time.

3.2 Analysis and Comparison of Experimental Results

In the same test environment, the system designed in this paper and the traditional binocular vision scanning system and the multi-vision scanning system were used to carry out the experiment. The scanning photos obtained in this paper are shown in Fig. 5:

Fig. 5. Partial scan results from the scanning system designed in this paper

The results from a traditional binocular scanning system are shown in Fig. 6:

Fig. 6. Partial scan results from traditional binocular vision scanning system

The results from a traditional multi-vision scanning system are shown in Fig. 7:

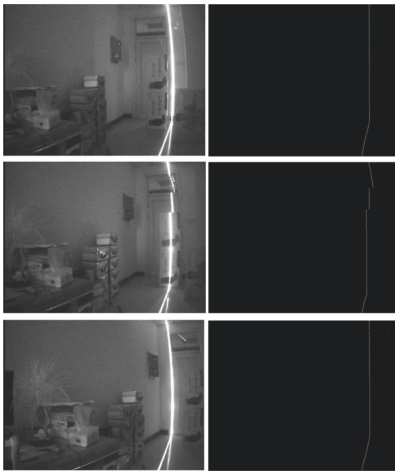

Fig. 7. Partial scan results from a conventional multivisual scanning system

From the results of the above three scans, it can be seen that there are a lot of burrs and defects in the center of the light stripe obtained by the traditional binocular scanning system and the multi-visual scanning system, which will affect the modeling accuracy in the later calculation.

At the center of the light strip, the distance from the surface of the space object illuminated by the light strip to the laser can be calculated by using the principle of triangulation, and a number of test points are selected for comparison. The test distance of the three systems is shown in Table 4:

Table 4. Comparison of distance measurement results (Unit: mm)

Test point serial number	Single camera scanning system designed in this paper	Traditional binocular vision scanning system	Traditional multivisual scanning system
1	2712.363	2538.978	2606.603
2	2768.491	2331.808	2708.700
3	2148.405	2186.134	2419.489
4	2590.905	2484.065	2497.770
5	2424.949	2495.316	2429.288
6	2491.978	2441.131	2166.875
7	2484.598	2628.465	2983.623
8	2326.824	2532.241	2193.066
9	2730.697	2292.340	2790.358
10	3053.439	2473.615	2769.631

(*continued*)

Table 4. (*continued*)

Test point serial number	Single camera scanning system designed in this paper	Traditional binocular vision scanning system	Traditional multivisual scanning system
11	2702.654	2964.539	2495.410
12	2471.716	2966.710	2761.785
13	2282.009	3036.451	2537.333
14	2147.153	2231.956	2821.215
15	2204.823	2940.512	2950.758
16	2423.309	2293.090	2176.451
17	2512.986	2274.348	2887.923
18	3004.273	2896.337	2569.137
19	2134.994	2183.157	2798.103
20	2303.156	2153.667	2306.675

The fitting value of the system is 0.973, the fitting value of the traditional binocular vision scanning system is 0.914, and the fitting value of the traditional multi-vision scanning system is 0.908. From the above results, we can see that the designed 3D laser scanning system based on artificial intelligence has higher precision and reliability than the two traditional scanning systems in point ranging.

When using 3D laser scanning system for 3D modeling, there will be many error factors, such as the error of laser scanning system itself, the error caused by the reflection of the scanned object, the error caused by the external environment and so on. The errors of the system itself are mainly caused by the performance defects of the instrument itself, including the laser fringe error is too thick, the camera has radial and tangential distortion; In addition, the errors caused by different material processes on the surface of the scanned object mainly include the errors caused by the roughness and inclination of the surface of the scanned object. In addition, the error caused by the external environment is mainly caused by the light.

4 Conclusion

In this paper, a single camera 3D laser scanning system based on artificial intelligence is proposed. The system can solve the problem of registration and matching errors in binocular/multi-vision 3D laser scanning system. Experimental results show that, compared with the two traditional systems, the system designed in this paper has the highest precision in scanning imaging distance, ranging curve fitting accuracy of 0.973. The scanning system proposed in this paper can meet the requirements of general users.

References

1. Xugang, L., Yinfei, C., Haifeng, H.: Application status and existing problems of 3D laser scanning technique in mine surveying in China. Metal Mine (03), 3540 (2019)
2. Junjie, M., Zhilong, L., Chengming, L., et al.: Research on visual collaborative design of complex rock foundation based on 3D laser scanning technology. Building Struct. **49**(21), 124–128 (2019)
3. Meng, W., Cuiyan, W., Huihui, D.: Virtual reconstruction system based on laser three-dimensional scanning building space structure. Laser J. **40**(11), 170173 (2019)
4. Mengyuan, S., Da-guang, H., Jieming, G., et al.: Road pavement deformation analysis method based on 3 D laser scanning point cloud. Sci. Technol. Eng. **19**(24), 386–391 (2019)
5. Ping, W., Chenxin, W., Xuan, Z.: Design and application of educational artificial intelligence system based on automation method. China Educ. Technol. **06**, 7–15 (2020)
6. Dongbo, Z., Zhuolin, W., Lixue, J.: Application of 3D laser scanning technology in defect detection of external wall thermal insulation system. Construct. Technol. **49**(09), 20–23 (2020)
7. Hongyu, M., Xin, Z.: 3D laser scanning technology and BIM technology in ancient building protection surveying and mapping. Geotechn. Eng. Technique **33**(04), 222–225 (2019)
8. Jun, L., Tao, G.: Application of new mobile 3D laser scanning technology in ellipsometry of shield segments. Bull. Survey. Mapp. **12**, 159–162 (2019)
9. Fuyin, Y., Hongyu, C., Tiejun, L., et al.: Research on monitoring and early warning and management system of leakage water based on 3D laser scanning subway operation tunnel. Construct. Technol. **48**(23), 76–79+128 (2019)
10. Hongquan, X., Yuetao, C., Fang, Z., et al.: Application of precise point positioning to the piggyback mobile laser scanning system. Eng. Surveying Mapping **28**(04), 60–63 (2019)
11. Liu, S., Liu, G., Zhou, H.: A robust parallel object tracking method for illumination variations. Mob. Netw. Appl. **24**(1), 5–17 (2018). https://doi.org/10.1007/s11036-018-1134-8
12. Liu, S., Fu, W., He, L., Zhou, J., Ma, M.: Distribution of primary additional errors in fractal encoding method. Multimedia Tools Appl. **76**(4), 5787–5802 (2014). https://doi.org/10.1007/s11042-014-2408-1
13. Hudson, R., Faraj, F., Fotopoulos, G.: Review of close-range three-dimensional laser scanning of geological hand samples. Earth Sci. Rev. **210**(1), 103321 (2020)
14. Lin, Y.M., Song, C., Rutledge, G.C.: Direct three-dimensional visualization of membrane fouling by confocal laser scanning microscopy. ACS Appl. Mater. Interfaces. **11**(18), 159–164 (2019)
15. Kiyono, T., Asawa, T., Oshio, H.: Laser-scanning-based method for estimating the distribution of the convective-heat-transfer coefficient on full-scale building walls. Bound.-Layer Meteorol. **178**(3), 1–24 (2021)
16. Feng, P., Zou, Y., Hu, L., et al.: Use of 3D laser scanning on evaluating reduction of initial geometric imperfection of steel column with pre-stressed CFRP. Eng. Struct. **198**(1), 109527.1–109527.12 (2019)
17. Long, J., Xiong, W., Wei, C., et al.: Directional assembly of ZnO nanowires via three-dimensional laser direct writing. Nano Lett. **12**(12), 59–63 (2020)
18. Duan, D., Podlesnik, J., Scharf, I., et al.: Fine sand particles enable antlions to build pitfall traps with advanced three-dimensional geometry. J. Exp. Biol. **223**(Pt 15), jeb.224626 (2020)
19. Tu, D., Xiao, G., Zhang, X., et al.: Laser stripe matching algorithm with coplanar constraint in underwater laser scanning systems. Optical Eng. **58**(11), 114108.1–114108.9 (2019)
20. Denk, W., Strickler, J.H., Webb, W.W.: Two-photon laser scanning fluorescence microscopy. Science (New York, N.Y.), **248**(4951), 73–76 (2019)

21. Hasselbach, J., Bogatscher, S., Rembe, C.: Laser scanner module with large sending aperture and inherent high angular position accuracy for three-dimensional light detecting and ranging. Opt. Eng. **58**(8), 087101.1–087101.13 (2019)
22. Zhao, Y., Spingler, F.B., Patel, Y., et al.: Localized swelling inhomogeneity detection in lithium ion cells using multi-dimensional laser scanning. J. Electrochem. Soc. **166**(2), 27–34 (2019)